

Gamut Mapping Adapted to Image Contents

R. Saito and H. Kotera

Department of Information and Image Sciences, Chiba University
Chiba, (Japan)

Corresponding author: R. Saito (saito@office.chiba-u.jp)

ABSTRACT

Gamut Mapping algorithm (GMA) between display and print images is a most typical application. Current GMA is mostly addressed to compress the out-of-gamut colours into the inside of printer gamut. Indeed, the highly saturated gamut images such as CG images on monitor are necessary to be compressed to make the appearance matching to print. However, the printer gamut has been much expanded with the improvements in printing media and devices. Hence, source image doesn't always fill the entire device gamut, and sometimes its' gamut need to be enlarged to get the better colour renditions. We have been proposed a Gamut Boundary Descriptor for comparing the gamut between image and device in discrete polar angle segment divided by ($\Delta\theta$, $\Delta\phi$) in CIELAB space. The gamut shell is described as the simple radial distances, called *r-image*.

This paper proposes a method of image-dependent gamut compression and expansion using histogram rescaling. The paper reports the experimental results in both compression for wide gamut and expansion for unsaturated narrow gamut. While, interest in hue uniformity has because of its importance when applied to gamut mapping. The color spaces used in the experiments were CIELAB, IPT, and CIECAM02.

1. INTRODUCTION

On the process of cross-media color reproduction, a key feature is to use the gamut mapping techniques to adjust the difference in color gamut between displays and printers. We proposed a *Image-to-Device (I-D) 3D Gamut Mapping algorithm (GMA)* by introducing the quick gamut comparison^{1, 2, 3}. To perform the 3D *I-D GMA* in effective, a simple and compact Gamut Boundary Descriptor (*GBD*) is necessary. We have been proposed a *GBD* for comparing the gamut between image and device in discrete polar angle segment divided by ($\Delta\theta$, $\Delta\phi$) in CIELAB space. The gamut shell is described as the simple radial distances, called *r-image*. This *GBD* represents a monochromatic 2D image whose pixel denotes the radial vector magnitude arranged in discrete integer address. This simple presentation makes it easy to compare the point-to-point gamut sizes between image and device. Current GMA is mostly addressed to compress the out-of-gamut colours into the inside of printer gamut^{4, 5}. Indeed, the highly saturated gamut images such as CG images on monitor are necessary to be compressed to make the appearance matching to print. However, the printer gamut has been much expanded with the improvements in printing media and devices. Hence, source image doesn't always fill the entire device gamut, and sometimes its' gamut need to be enlarged to get the better colour renditions. We presented a method of image-dependent gamut compression using *r-image* and introduced image-dependent gamut expansion using histogram stretch⁶. The numerical gamut comparison by *r-image* to decide compression or expansion is not easy way at present because all image gamut is not out of device gamut but also not inside of that.

This paper proposes a method of image-dependent gamut compression and expansion using histogram rescaling. A histogram rescaling in reference to the each *GBD* of image and device is automatically applied for gamut mapping.

2. HISTOGRAM RESCALING USING GBD

We have developed an automatic gamut extraction algorithm from a random color map. The source image in the CIELAB space are segmented by a constant polar angle step, that is, $\Delta\theta$ in hue and $\Delta\phi$ in sector. The gamut center was set at a neutral point $[L^*_0, a^*_0, b^*_0] = [50, 0, 0]$.

$$\begin{aligned} \begin{bmatrix} L^* \\ a^* \\ b^* \end{bmatrix} &= \tan^{-1} \begin{bmatrix} b^* \\ a^* \end{bmatrix} \begin{bmatrix} L^* \\ a^* \\ b^* \end{bmatrix} \\ \begin{bmatrix} L^* \\ a^* \\ b^* \end{bmatrix} &= \tan^{-1} \begin{bmatrix} L^* \\ (a^*)^2 + (b^*)^2 \end{bmatrix}^{1/2} \end{aligned} \quad (1)$$

We define the radial matrix \mathbf{r}_{gamut} whose element is given by the maximum radial vector in each polar angle segment. The magnitude of radial vector \mathbf{r}_{jk} is given by the norm

$$\|\mathbf{r}_{jk}\| = \left[(L^*_{jk})^2 + (a^*_{jk})^2 + (b^*_{jk})^2 \right]^{1/2}. \quad (2)$$

We proposed to replace the 3-D radial vectors to 2-D distance array arranged in rectangular lattice point (j, k) , named **r-image**^{1, 2, 3}.

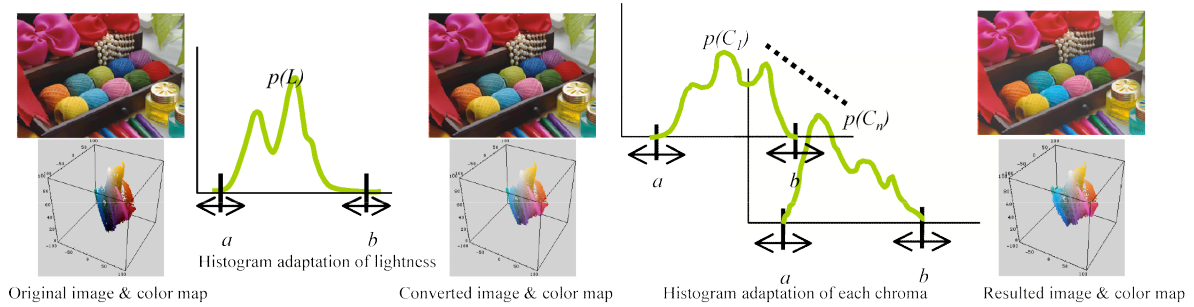


Figure 1: Schema of gamut mapping model based on histogram rescaling.

In order to perform natural and pleasant gamut adaptation automatically, we propose an image gamut rescaling method based on the histogram stretching. The histogram rescaling method can easily adapt the image gamut to target device gamut setting corresponding lowest value and highest value. Fig.1 illustrates an explanatory model to gamut mapping based on the histogram rescaling. The histogram rescaling automatically applies the degraded image and compresses the saturated image to the natural and pleasant images. The histograms of lightness and chroma are adapted separately in CIELAB space as the following steps. (1) RGB to LAB conversion, (2) Histogram rescaling for lightness component, (3) Segmentation of chroma component, (4) Histogram rescaling for chroma component. In the original histogram $p(L)$, lowest value a and highest value b are expanded or compressed to target device gamut histogram using equation (3).

$$p(L) = (T_h - T_l) \frac{p(L) - a}{b - a} + T_l \quad (3)$$

Where T_h and T_l are denote higher point and lower point of target device.

After the histogram rescaling of L , the chroma components are segmented into m divisions by ΔH in hue angle H . Then chroma C of each division is expanded or compressed by histogram rescaling as same as L without changing color hue.

Fig.2 shows resulted images by gamut mapping using histogram rescaling. The printer gamut is obtained from the measurements of color chips printed on superfine paper using an Epson 6-color dye Ink-jet printer. XYZ tristimulus values of the printed chips are measured with a Gretag spectrophotometer. Fig. 2-a) is a degraded original image and its color map. Fig.2-c) is a saturated original image and its color map. Both images were mapped to gamut of Ink-jet printer. Each image result and color map are shown Fig. 2-b) and 2-d). The chroma was segmented to 16 ΔH division. The degraded image was dramatically improved to comfortable image with the bright and vivid colors. The saturated image was also well compressed in printer gamut.

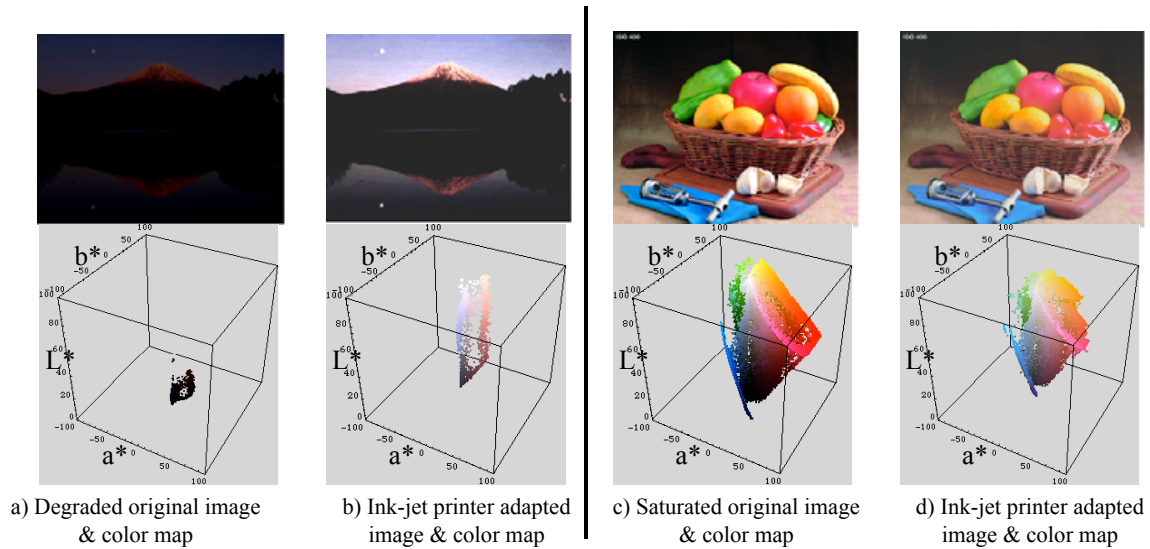


Figure 2: Result of histogram rescaling for degraded and saturated images.

3. UNIFORM COLOR SPACE

It is desirable for the gamut mapping to be performed in a totally perceptual uniform color space. Uniform color space CIELAB recommended by CIE was intended so that Munsell colors are distributed uniformly and MacAdam's ellipses are transformed into equal radius circles as much as possible. However, some of the experiments indicated that color spaces were not perfectly uniform⁷. Significant perceived hue shifts can result depending on chroma compression and expansion. The most notable example occurs in the "blue" region of color space where a chroma "blue" is mapped to a chroma "purple" when mapped along lines of constant CIELAB metric hue angle⁸. In 1997, the CIECAM97s color appearance model was proposed to extend the traditional color spaces. The CIE Technical Committee 8-01 has recently proposed a single set of revisions to the color appearance model. The CIECAM02 color appearance model builds upon the basic structure and form of the CIECAM97s color appearance model⁹. On the other hand, Ebner and Fairchild developed a new color space (named IPT) based on Hung and Berns' and Braun, Ebner and Fairchild's experimental data set. This color space was made to have perceptual hue lines as straight as possible¹⁰. The lightness dimension is denoted as I , the red-green dimension is denoted as P , and the yellow-blue dimension is denoted as T .

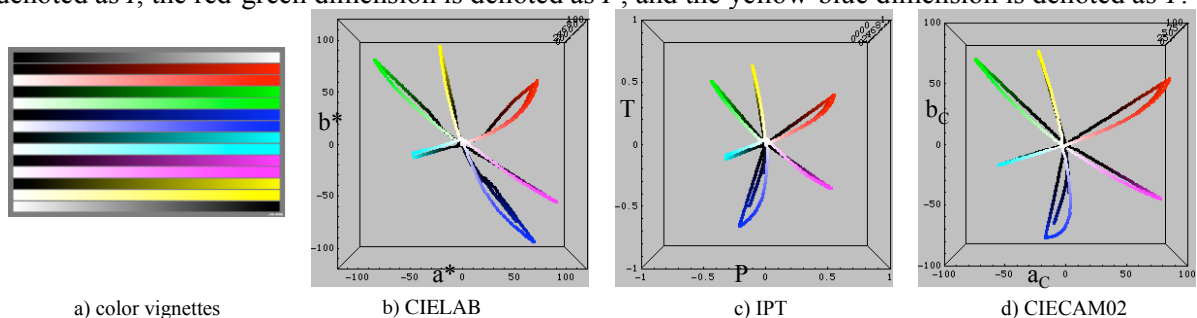


Figure 3: Plot of color vignettes data in each color spaces

Fig.3 shows plot of color vignettes data in each color spaces. Fig. 2-a) is a original image, Fig. 3-b) is a CIELAB a^*-b^* view, Fig. 3-c) is a IPT $P-T$ view, and Fig. 3-d) is a CIECAM02 a_c-b_c view. The linearity of hue loci in each color spaces especially has a curvature at blue locus. In CIELAB color space, loci of blue and purple are very close, and blue locus is curved toward purple. On the other hand, in IPT and CIECAM02 color space, each hue loci has been distributed evenly in the color space.

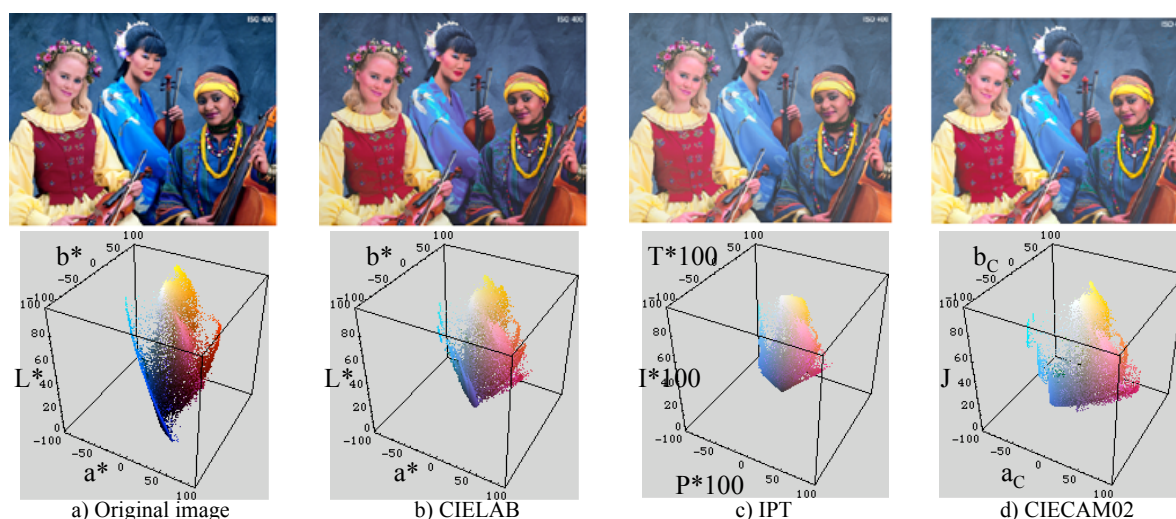


Figure 4: Result of histogram rescaling for saturated images at each color spaces.

Fig.4 shows resulted images and color maps by gamut mapping using histogram rescaling at each color spaces. In CIELAB color space, clothes of women in middle and right were changed blue to purple. However, in IPT and CIECAM02 color space, these clothes were kept blue. The chroma of entire image was more vivid in CIECAM02 color space than in IPT's. The color space for gamut mapping was better performed in CIECAM02 than in CIELAB and IPT, in other some images too.

4. CONCLUSIONS

We proposed histogram rescaling for gamut mapping in reference to the each **GBD** of image and device. This model is automatically applied an expansion of degraded images and a compression of saturated images. The CIECAM02 color space was better performed for gamut mapping than other color spaces. Future works will be continued to apply for gamut mapping on the various devices.

References

1. R. Saito and H. Kotera, "Extraction of Image Gamut Surface and Calculation of its Volume", Proc. 8th IS&T/SID CIC, pp.330-333 (2000).
2. R. Saito and H. Kotera, "3D Gamut Mapping by Comparison between Image and Device Gamut Description", Proc. ICIS'02, TOKYO, pp.407-408 (2002).
3. R. Saito and H. Kotera, "Image-dependent three-dimensional gamut mapping using gamut boundary descriptor", Jour. Elect. Imaging, 13 (3) pp. 630-638 (2004).
4. J. Morovic and M. R. Luo, "Evaluating Gamut Mapping Algorithms for Universal Applicability", *Col. Res. Appl.* 26, pp.85-102 (2001).
5. L. W. MacDonald and M. R. Luo, *Color Imaging*, John Wiley & Sons (1999).
6. R. Saito and H. Kotera, "A Versatile 3D Gamut Mapping Adapted to Image Color Distribution", Proc. IS&T's NIP20, pp.647-651 (2004).
7. N. Kato, M. Ito and S. Ohno, "Three-dimensional gamut mapping using various color difference formulae and color spaces", Jour. Elect. Imaging, 8 (4) pp. 365-379 (1999).
8. G. J. Braun and M. D. Fairchild, "Gamut Mapping for Pictorial Images", TAGA Proceedings, pp.645-660 (1999).
9. N. Moroney, M.D. Fairchild, C. Li, M.R. Luo, R.W.G. Hunt and T. Newman, "The CIECAM02 Color Appearance Model", Proc. 10th IS&T/SID CIC, pp.23-27 (2002).
10. F. Ebner and M. D. Fairchild, "Development and Testing of a Color Space (IPT) with Improved Hue Uniformity", Proc. 6th IS&T/SID CIC, pp.8-13 (1998).